Alpine structural evolution of the Internal Piedmont Zone in the Upper Viù Valley (Lanzo Valleys Ophiolite, Western Alps)

Marcello De Togni[1], Marco Gattiglio[1], Gianni Balestro[1] & Matthieu Roà[1]

[1] Earth Sciences Department, University of Torino, Via Valperga Caluso 35, I-10125 Torino, Italy.

MDT, 0000-0003-4143-0747; MG, 0000-0002-1885-2872; GB, 0000-0001-5215-4659; MR, 0000-0003-1767-5947.

Rend. Online Soc. Geol. It., Vol. 60 (2023), pp. 16-23, 4 figs., https://doi.org/10.3301/ROL.2023.27

Short note

Corresponding author e-mail: marcello.detogni@unito.it

Citation: De Togni M., Gattiglio M., Balestro G. & Roà M. (2023) - Alpine structural evolution of the Internal Piedmont Zone in the Upper Viù Valley (Lanzo Valleys Ophiolite, Western Alps). Rend. Online Soc. Geol. It., 60, 16-23, https://doi.org/10.3301/ROL.2023.27.

Guest Editor: Alberto Corno

Submitted: 23 November 2022

Accepted: 17 February 2023

Published online: 18 April 2023

SOCIETÀ GEOLOGICA ITALIANA
FONDATA NEL 1881 - ENTE MORALE R. D. 17 OTTOBRE 1885

ABSTRACT

New structural data have been collected in the high-pressure meta-ophiolites exposed in the Lanzo Valleys (*i.e.*, the Lanzo Valleys Ophiolite, LVO) and tectonically overlying the continental crust of the Dora-Maira and Gran Paradiso massifs in the Western Alps. Detailed geological mapping and structural analysis carried out in the south-western sector of the LVO (*i.e.*, the Upper Viù Valley) allow to distinguish four ductile deformation phases, corresponding to the subduction-related D1 phase, the early exhumation-related D2-phase and the late exhumation-related D3 and D4 phases. The geometry of structures and kinematics have been reconstructed, and their regional tectonic meaning is discussed in the frame of the Alpine tectonic evolution of the Internal Piedmont Zone (*i.e.*, the remnants of the Alpine Tethyan oceanic lithosphere) in the Western Alps.

KEY-WORDS: Piedmont Zone, ophiolite, Alpine tectonic, structural analysis, Lanzo valleys.

INTRODUCTION

The Western Alpine meta-ophiolites are the remnants of the Alpine Tethyan oceanic lithosphere (*i.e.*, the Piedmont Zone; *e.g.*, Dal Piaz et al., 2003), and consist of different tectonic units stacked in the Alpine orogenice wedge (Fig. 1). In the last fifteen years, most of these tectonic units were thoroughly investigated (*e.g.*, Agard, 2021, Festa et al., 2021, and references therein), but the high-pressure meta-ophiolites exposed in the Lanzo Valleys (*i.e.*, the Lanzo Valleys Ophiolite; LVO) are presently poorly studied. After the key-work of Nicolas (1969), further comprehensive studies about the LVO were not carried out.

This paper is part of a wider project, which aims to give new modern knowledge about both the pre-orogenic (*i.e.*, oceanic) tectonostratigraphy and the Alpine tectono-metamorphic evolution of the LVO. New structural data are presented in order to outline the polyphase structural evolution of the LVO in the Upper Viù Valley (Fig. 2). Structural analysis and geological mapping allow distinguishing four different deformation phases recorded by the meta-ophiolite succession, which is also briefly described. The regional tectonic meaning of these deformation phases is discussed in the frame of the Alpine tectonic evolution of the Piedmont Zone in the Western Alps.

GEOLOGICAL SETTING

The Western Alps (Fig. 1) originated from the collision between the European and Adriatic Plates after the closing of the interposed Alpine Tethys (*i.e.*, the Ligurian-Piedmont oceanic basin; *e.g.*, Rosenbaum & Lister, 2005; Handy et al., 2010). The latter developed through Middle to Late Jurassic seafloor mantle exhumation and (ultra)slow-spreading processes (*e.g.*, Manatschal & Müntener, 2009; Balestro et al., 2019). During subsequent plates convergence, remnants of the Alpine Tethyan oceanic lithosphere (*i.e.*, the Piedmont Zone; *e.g.*, Dal Piaz et al., 2003) were tectonically sandwiched in between different continental crust units derived from the Europe and Adria-related distal margins.

The different Alpine meta-ophiolite units were affected by pervasive deformation associated with Paleocene to Middle Eocene subduction-related metamorphism, ranging from blueschist- to eclogite-facies P-T peak conditions (Agard, 2021,

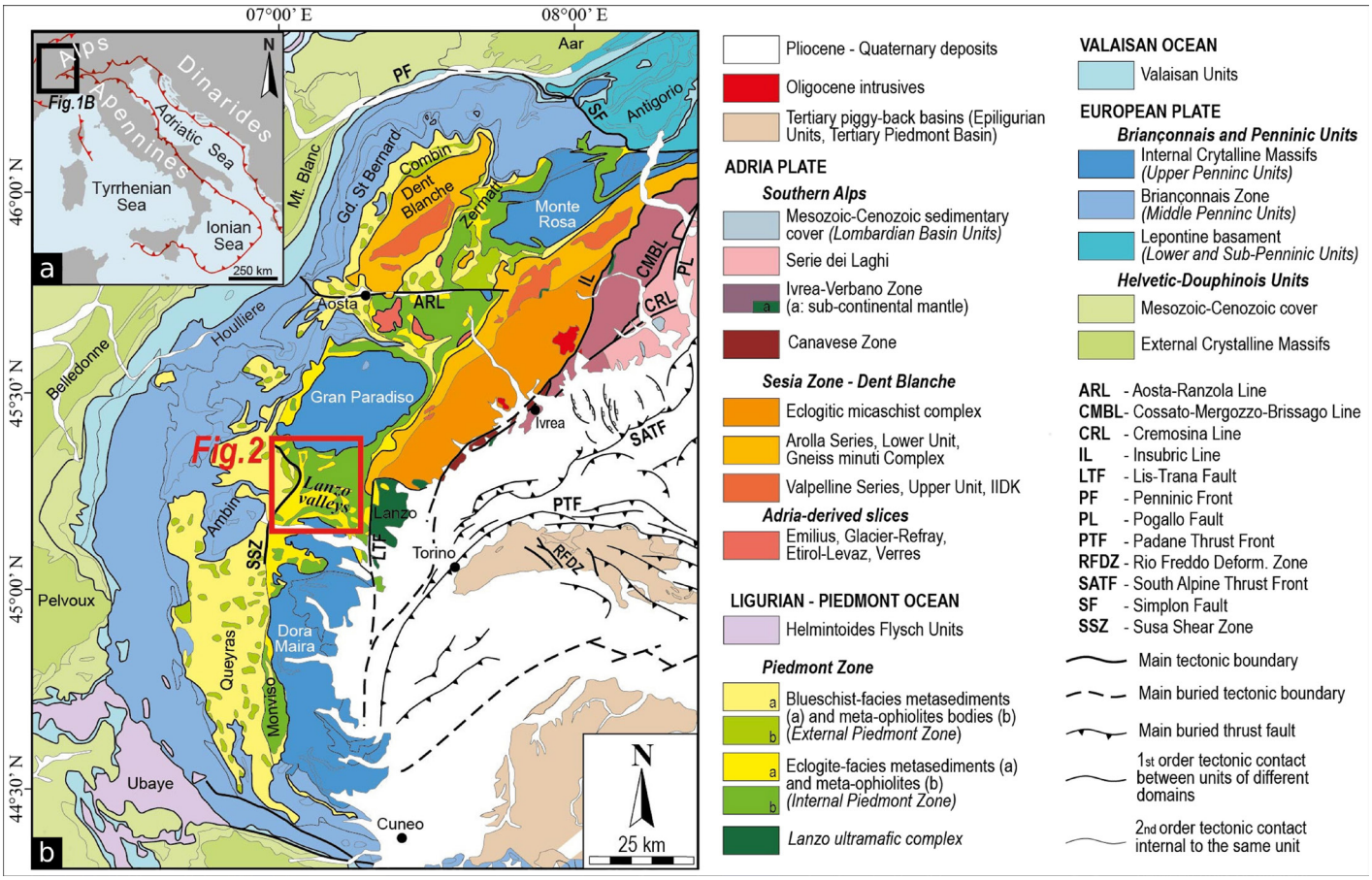

Fig. 1 - (a) Sketch of the Alps-Apennine orogenic system and location of the map. (b) Tectonic map of the Western Alps (modified from Balestro et al., 2022) with location of map shown in Fig. 2 (red square).

and references therein). They have been classically distinguished into two groups: (i) the eclogite-facies Internal Piedmont Zone (*i.e.*, the Zermatt-Saas Zone *Auct.*, Bearth, 1967), mainly consisting of meta-ophiolite successions with minor oceanic metasediments (Balestro et al., 2018; Rebay et al., 2018; Tartarotti et al., 2019; Festa et al., 2021, and references therein); (ii) the blueschist-facies External Piedmont Zone (*i.e.*, the Combin Zone *Auct.*, Bearth, 1967), made up of a thick succession of Cretaceous pelagic metasediments hosting scattered meta-ophiolite bodies (Tricart & Schwartz, 2006; Herviou et al., 2021, and references therein).

The meta-ophiolite units belonging to the Internal Piedmont Zone tectonically overlay the Europa-derived Internal Crystalline Massifs (Gasco et al., 2011, and references therein), and in particular, the LVO occurs in between the Dora-Maira Massif (to the S) and the Gran Paradiso Massif (to the N). The LVO is laterally bounded by the Susa Shear Zone (Ghignone et al., 2020b), separating the LVO from the External Piedmont Zone (to the W), and by the Lis-Trana Fault (Balestro et al., 2009), separating the LVO from the Lanzo Ultramafic Complex (to the E) (Fig. 1). The Susa Shear Zone was characterized by two different shearing events (T1 and T2; Ghignone et al., 2020b). T1 occurred during early exhumation and was characterized by "apparent reverse" Top-to-E kinematics, whereas T2 occurred during late exhumation and was characterized by Top-to-W kinematics.

The LVO succession consists of (i) serpentinite enclosing metagabbro bodies, (ii) metabasalt and mafic metabreccia, and (iii) metasediments (quartzite, marble and calcschist) (Nicolas, 1969; Leardi & Rossetti, 1985; De Togni et al., 2021). This meta-ophiolite succession was pervasively deformed during different deformation phases (Perotto et al., 1983; Spalla et al., 1983). The eclogite-facies metamorphic peak conditions were achieved at middle Eocene times (~41-46 Ma; Ghignone et al., 2021b), and followed by greenschist-facies re-equilibration (Sandrone et al., 1986; Plunder et al., 2012; Ghignone et al., 2021a).

METHODS

Geological and structural data were collected during fieldwork carried out at 1:5,000 scale, over an area of about 40 km^2. The different deformation phases and their relative chronology have been distinguished through overprinting and crosscutting relationships among the different structural elements (foliations, lineations, folds), and by their geometries, styles, interference patterns and senses of shear. Statystical analysis of data was carried out through stereographic plots using *OpenStereo 2.0b* software. It allow us to identify both clusters, scatterings, mean values, best-fit planes and theoretical folding axes (π). The orientations are given in *dip direction/dip* for planes, *trend/plunge* for lines.

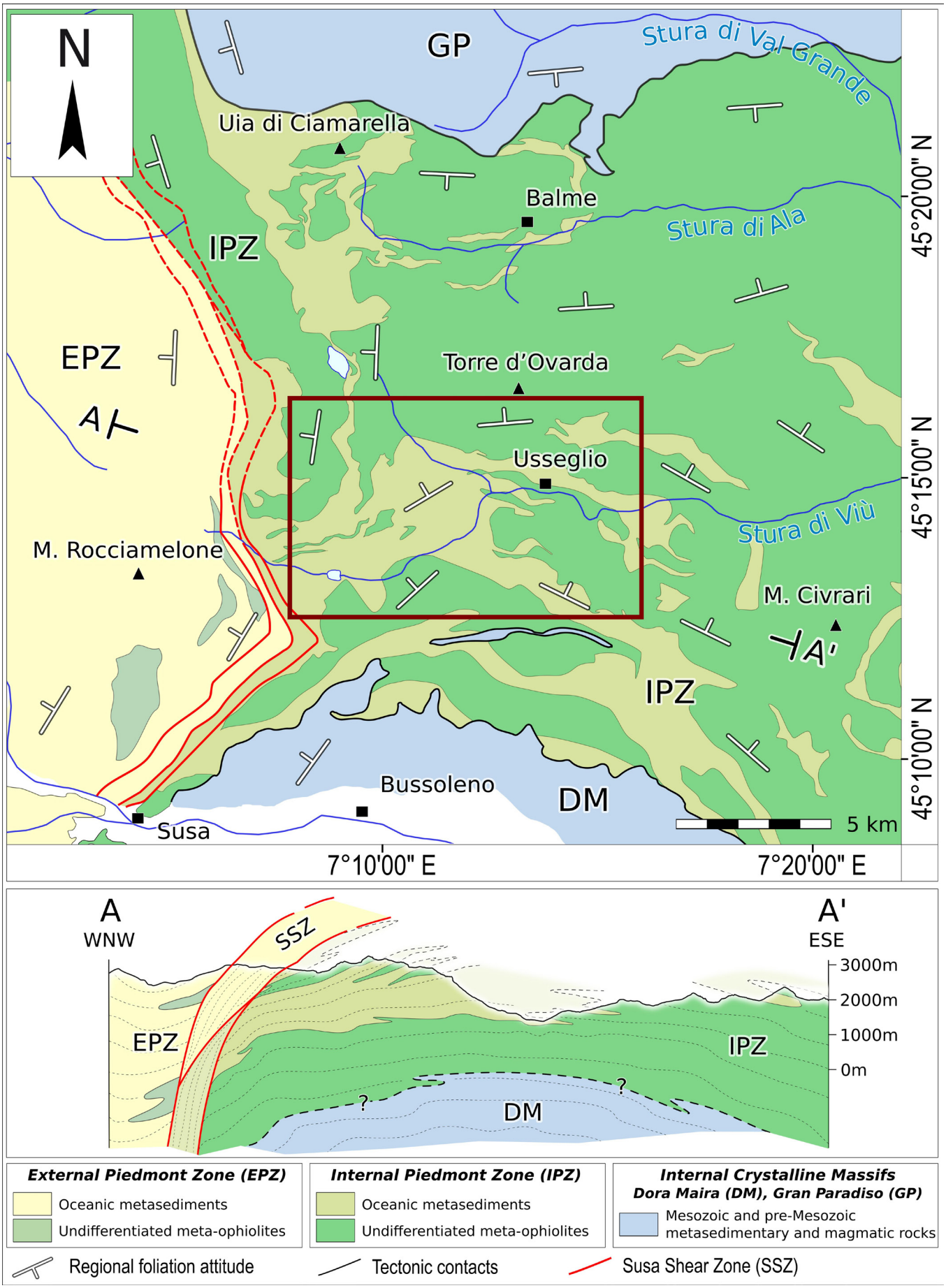

Fig. 2 - Structural sketch map of the Lanzo Valleys area (modified from Nicolas, 1969, Perotto et al., 1983, Bigi et al., 1990, Ghignone et al., 2020a); red square indicates the study area.

LITHOSTRATIGRAPHY

The LVO succession in the Upper Viù Valley consists of serpentinite, metagabbro, metabasalt, mafic metasandstone and metabreccia, quartzite, marble and calcschist (see details in De Togni et al., 2021).

The serpentinite is generally massive and up to hundreds of meters thick, and locally passes to serpentine-schist, talcschist and meta-ophicarbonate layers. The serpentinite embeds up to few meters thick metagabbro bodies and rodingitic/gabbroic dykes, which are both of Mg-Al-rich and Fe-Ti-rich composition. The metabasalt mainly consists of banded metabasite and prasinite, and locally displays relicts of primary igneous textures such as pillow-lavas. The metabasalt is characterized by strong thickness variations, from few meters up to hundreds of meters. Ovardite (*i.e.*, rock mainly made up of albite, chlorite and carbonate; Leardi & Rossetti, 1985) and rare chlorite-schist also occur. The metasandstone and metabreccia are represented by decimeter-thick horizons, consisting of angular to sub-rounded clasts of mafic composition, up to centimeters in size, embedded in a fine-grained carbonate-bearing mafic matrix. In different sectors of the study area, the mantle rocks and the hosted metagabbro, are stratigraphically overlain by (i) metabasalt, (ii) mafic metabreccia or (iii) carbonate metasediments, highlighting the original existence of an articulated seafloor tectonostratigraphic architecture.

The above-described lithostratigraphy is overlain by the supra-ophiolitic metasedimentary cover which, at its bottom, is represented by quartzite passing to basal meta-chert, micaceous quartzite and quartz-micaschist. The quartzite is characterized by a thickness variation (up to few meters), which roughly follows that of metabasalt. It gradually passes upward to a discontinuous gray marble, which consists of thin (few meters) carbonate-rich layers. The marble in turn passes upward to hundreds of meters thick carbonate-rich calcschist, calcschist and phylladic calcschist.

STRUCTURAL ANALYSIS

Mesoscale structural observations (Fig. 3), together with structural-statystical analysis (Fig. 4), allowed to distinguish four ductile deformation phases (from D1 to D4), which affected the above described meta-ophiolite succession. The resulting structural architecture is summarized in a 3D structural block-model (Fig. 4g).

D1 phase

The D1 is the oldest deformation phase and is mainly represented by the relict S1 foliation. The latter is locally preserved in the rheologically stronger rocks (*i.e.*, metagabbro, quartzite and marble; Figs. 3a,b,c), as a millimeter-scale metamorphic layering. The S1 surfaces are characterized by the occurrence of a L1 stretching mineralogical lineation.

The S1 is parallel to the axial plane of rarely observed D1 isoclinal folds, with acute and "flame-shaped" hinges (Figs. 3a,b), showing non-cylindrical geometries (anvil-shaped and cat's-eye-shaped folds; Fig. 3b).

The S1 is preserved in D2 fold hinges (Fig. 3c), whereas it is parallel to S2 along D2 fold limbs (Figs. 3b, 4a,b), showing a "composite fabric" (S1+S2). Along S1-parallel marble layers, asymmetrical boudins and S-C structures are also developed.

The S1 foliation mainly dips towards N at medium angle (Fig. 4a) but it is scattered along a NNW-striking best-fit great circle. The latter returns a low-angle ENE-plunging theoretical folding axis (π), roughly consistent with the effects of superposed D2- and D3-folding (see below). Both L1 lineation and A1 axes are mainly N-plunging (Fig. 4c), but also scattered by subsequent deformation phases.

D2 phase

The D2 represents the most evident deformation phase and it is characterized by the development of the S2 regional foliation.

D2 folds show isoclinal to tight profile and rounded hinges (Fig. 3b,c). Cuspate-lobate geometries and boudinage processes developed along contacts between rocks with different rheological behavior (marble-calcschist or metagabbro-serpentinite).

The S2 corresponds to a pervasive foliation, which almost parallelize the S1 foliation. However, comparison between plots of Figs. 4a and 4b highlights that a small variation in orientation still occur between S1 and S2 (also visible in Fig. 3a).

The S2 foliation is parallel to the axial plane of the D2 folds, mainly dipping toward N at medium angle (Fig. 4b), but it is scattered along a NNE-striking best-fit great circle. The latter returns a low-angle WNW-plunging theoretical folding axis (π), consistently with D3 folding axes (see below).

Furthermore, the weak E-W directed scattering of S2 poles seems to be consistent with deformation related to the D4 phase.

L2 mineralogical stretching lineations occurring on the S2 surfaces are mainly W-plunging at low angle (Fig. 4c). Similar orientations result from A2 axes and intersection lineations between S1 compositional banding and S2 (Figs. 4c,d). This overlapping between orientations of L2 lineations and A2 axes, is consistent with the development of non-cylindrical folds during the D2 phase, highlighted by the occurrence of eye-shaped, anvil-shaped and cat's-eye-shaped mesoscale folds (Fig. 3c).

Along the S2 foliation rotated porphyroclasts, S-C structures, and minor asymmetric boudins, indicate a top-to-W sense of shear (Fig. 3d), outlining the westward vergence of this deformation phase. The D2 and D1 folds are coaxial and produced an interference pattern (Fig. 3b) of "type 3" (according to the classification of Ramsay, 1962).

D3 phase

The D3 deformation phase develops parallel open to close folds with rounded hinges (Figs. 3e,f). They show short limb-long limb geometry, defining asymmetrical folding with sub-vertical and partly overturned short limbs (Fig. 3f), and northward vergence. Locally, asymmetric box folds with conjugate axial planes occur.

D3 folds, in the rheologically weaker rocks (*i.e.*, serpentine-schist, talc-schist, prasinite and more phylladic calcschist) locally develops an S3 axial plane foliation, which corresponds to a

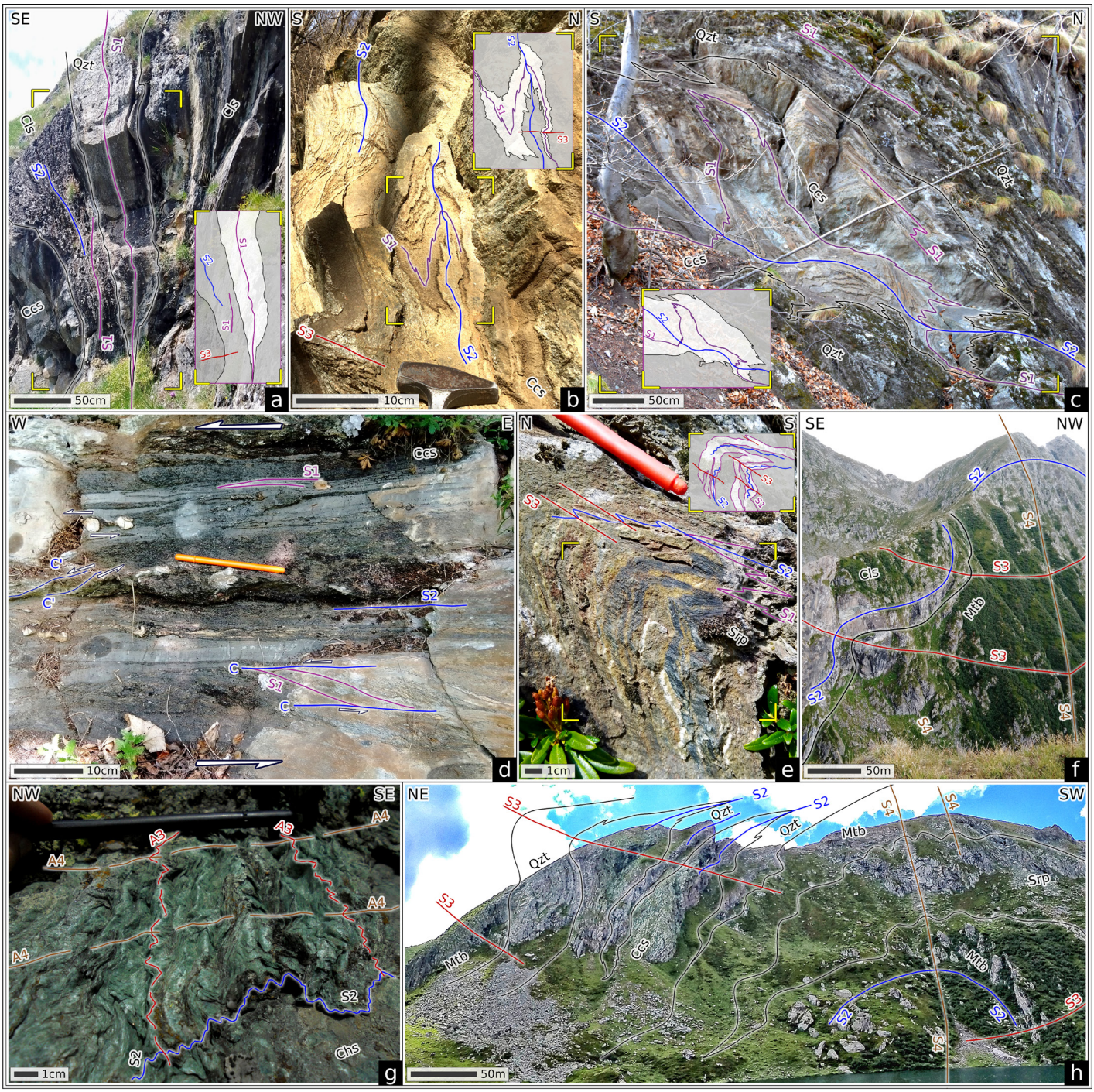

Fig. 3 - Field photographs of D1 to D4 mesoscale structures and their relationships, from the study area. (a) D1 isoclinal sinformal anticline fold in quartzite (Qzt) within calcschist (Cls) and carbonate-rich calcschist (Ccs). Note the very acute D1 hinge and the angular relationship between S1 (in purple) and S2 (in blue) foliations. Also, D3 folds (S3 axial plane in red) occur. (b) D1 eye-shaped sheath fold (S1 axial plane in purple) in a marble layer within carbonate-rich calcschist (Ccs), deformed by isoclinal D2 folds (S2 axial plane, parallel to the S2 foliation, in blue) and later D3 open folds (S3 axial plane in red). The D1-D2 interference pattern is "type 3". (c) Carbonate-rich calcschist (Ccs) in the core of a large-scale D2 anvil-shaped sheath fold, sorrounded by micaceous quartzite (Qzt) and displaying opposite closures along the same axial plane (S2 axial plane in blue); observed section perpendicular to the L2 lineation. Calcschist also represents the core of a D1 syncline (S1 axial plane in purple). Micaceous quartzite displays an S2 foliation, while the folded surface of carbonate-rich calcschist is an S1 foliation (in purple), parallel to the compositional banding. (d) High-strain mylonitic band within the carbonate-rich calcschist along the S2 foliation (in blue); the observed surface approximates the XZ plane of the strain ellipsoid. C planes (in blue) deflecting S1 foliation, asimmetric strain shadows of porphyroclasts of former calcite veins, and C' (in blue) high-angle extensional planes define a top-to-W sense of shear. Drag folding of S1 also occurs. (e) D3 closed fold in serpentinite (Srp), developing a pervasive S3 crenulation cleavage (in red), parallel to the fold axial plane. The S1 foliation (in purple), is deformed by isoclinal D2 folds (S2 foliation/axial plane in blue), realizing a "type 3" interference pattern (according to the classification of Ramsay, 1962). (f) Panoramic view showing the calcschist (Cls) and metabasalt (Mtb) contact, parallel to the SE-dipping S2 foliation (in blue), folded by a D3 synform-antiform couple (S3 axial planes in red). D3 short limbs are slightly overturned. Northwestward, S2 dips to the NW, defining a big-scale D4 antiform. (g) Chlorite-schist (Chs) layer, within metabasalt, displaying a pervasive S2 foliation (in blue) and two intense crenulations as an effect of D3 and D4 superimposed folding. A4 axes (in brown) are perpendicular to A3 axes (in red), realizing a "type 1" interference pattern (according to the classification of Ramsay, 1962). (h) Panoramic view showing a huge D4 antiformal fold involving an already structured (S2 axial planes in blue, S3 axial planes in red) "complete" lithostratigraphic section (serpentinite, Srp, metabasalt, Mtb, quartzite, Qzt, and calcschist, Ccs). Note the several D4 parasitic folds in the hinge zone within serpentinite.

millimeter-spaced crenulation cleavage (Fig. 3e,g). In turn, in the rheologically stronger rocks, S3 consists of a centimeter-spaced disjunctive cleavage, often refracted along the fold profile.

S3 axial planes are on average sub-horizontal (Fig. 4e) and they are weakly scattered along a E-striking best-fit great circle, corresponding to a low-angle S-plunging theoretical folding axis (π), The latter is consistent with deformation related to the D4 phase. A3 axes are on average E-W trending and mainly W-plunging at low angle (Fig. 4f), and their minor E-dipping attitude is likewise due to effects of D4 phase. A3 axes are not uniformly oriented in the studied area. They are mostly NE-SW trending in the western sector of the study area (Fig. 2), and mostly WNW-ESE trending in the eastern sector. The D3 and D2 folds result roughly coaxial and realized an interference pattern (Fig. 3b) of "type 3" (Ramsay, 1962).

D4 phase

The D4 deformation phase develops large-wavelength folds (Figs. 3f,h), mostly highlighted by large-scale variations of the S2 foliation (Fig. 2). The D4 folds show gentle to open profiles, parallel geometry and very rounded hinges. Mesoscale D4 folds are scarce but crenulation fold hinges (Fig. 3g) and S4 disjunctive cleavage associated to veins, locally developed.

A4 axes are mainly N-S trending whereas D4 axial planes are almost N-S striking and dipping both toward E and toward W at high angle. In large-scale D4 hinges, wherein several parasitic folds occur, "type 1" interference patterns (Ramsay, 1962) with D3 structures can be observed (Fig. 3g,h).

DISCUSSION

Observations of mesoscale structures and structural analysis allowed to distinguish four deformation phases (Fig. 4g), whose regional meaning can be discussed into the frame of the tectonic evolution of the LVO (Fig. 2). The different deformation phases are the result of the Alpine subduction-exhumation cycle recorded by the LVO, as also described outside the studied area in other sectors of the LVO (Perotto et al., 1983; Spalla et al., 1983; Ghignone et al., 2020b; Caso et al., 2021).

The D1 phase, as resulting by "flame-shaped" hinge fold geometries and by nearly parallelism between L1 stretching lineations and A1 axes, was characterized by non-cylindrical folding (Fig. 4g) developed under deformation regime with significant simple shear component. At a large scale, the inferred tectonic transport direction is approximately N-S trending (Gasco et al., 2011). The S1 foliation developed at eclogite-facies metamorphic peak conditions (Spalla et al., 1983; Plunder et al., 2012; Ghignone et al., 2021a), in middle Eocene times (~41-46 Ma; Ghignone et al., 2021b). The D1 phase takes place during the transition between subduction of the LVO and the beginning of exhumation, when the LVO was early coupled with the underlying Dora Maira Massif (Gasco et al., 2011).

Similarly to D1, the D2 phase was characterized by non-cylindrical folding (Fig. 4g) (Fig 4g) under significant simple shear regime but geometries of folds appear to be more strongly constrained by occurrence of rocks with different rheological behaviour. Kinematic indicators along the S2 foliation indicate a top-to-W sense of shear, coeval with the widespread westward transport of nappes in the Western Alps (*e.g.*, Tricart & Schwartz, 2006). The S2 foliation developed at ~40-36 Ma (Ghignone et al., 2021b), during metamorphic re-equilibration under greenschist facies conditions. The S2 foliation was nearly coeval with the mylonitic foliation developed along the Susa Shear Zone (Fig. 2), which drove exhumation of Internal Piedmont Zone and its tectonic juxtaposition with External Piedmont Zone (*i.e.*, the T1 tectonic event of Ghignone et al., 2020b).

The D3 phase was characterized by N-verging folding (Fig. 4g) and was associated with late exhumation of the LVO under greenschist-facies conditions (Gasco et al., 2013). The D3 phase was tectonically linked with early development of dome-like structures in the Dora Maira and Gran Paradiso massifs, which underlie the IPZ. The dispersion of A3 axes, which cannot be related to the effects of the subsequent D4 phase, can be explained taking in mind that the studied area is located close to the northern edge of the Dora Maira Massif (Fig. 2). The latter is well defined by deflection of the composite regional foliation (*i.e.*, S1+S2), whose strike orientations, moving from eastern to western sectors, vary from NW-SE, to E-W and NE-SW directions (Fig. 2). The D3 folds seem to follow the same trend with a "centrifugal" vergence, parallel to the edges of the dome itself.

The D4 phase developed at shallow crustal levels, at the transition between ductile and brittle conditions. The D4 folds accommodated a later phase of dome-related uplift of the Dora-Maira and Gran Paradiso massifs, following the same trend of D3 folds and with tectonic transport outward from the dome. The D4 phase was coeval with a second tectonic event along the Susa Shear Zone (*i.e.*, the T2 of Ghignone et al., 2020b), developing westward extensional shear zones along short limbs of D4 folds.

CONCLUSIONS

Fieldwork and structural analysis allow us to depict the deformation strain pattern affecting the meta-ophiolite succession in the Upper Viù Valley. The Alpine tectonic evolution of the LVO has been discussed in the light of the obtained data and by comparison with existing tectonic models for the subduction and exhumation stages of the IPZ.

The reconstruction of the geometry of structures and their kinematics in the study area has a twofold key role. It allows us to improve knowledge about subduction and exhumation processes involving the IPZ, but it is also needed to detect pre-Alpine tectono-stratigraphy and oceanic reconstruction of the Western Tethys.

Further investigations about the geology of the whole LVO will be aimed to (i) investigate more in depth the complex deformation settings possibly resulting from sheath folds (see Maino et al., 2021), (ii) realize detailed and modern geological maps and (ii) detect the microscale blastesis-deformation relationships.

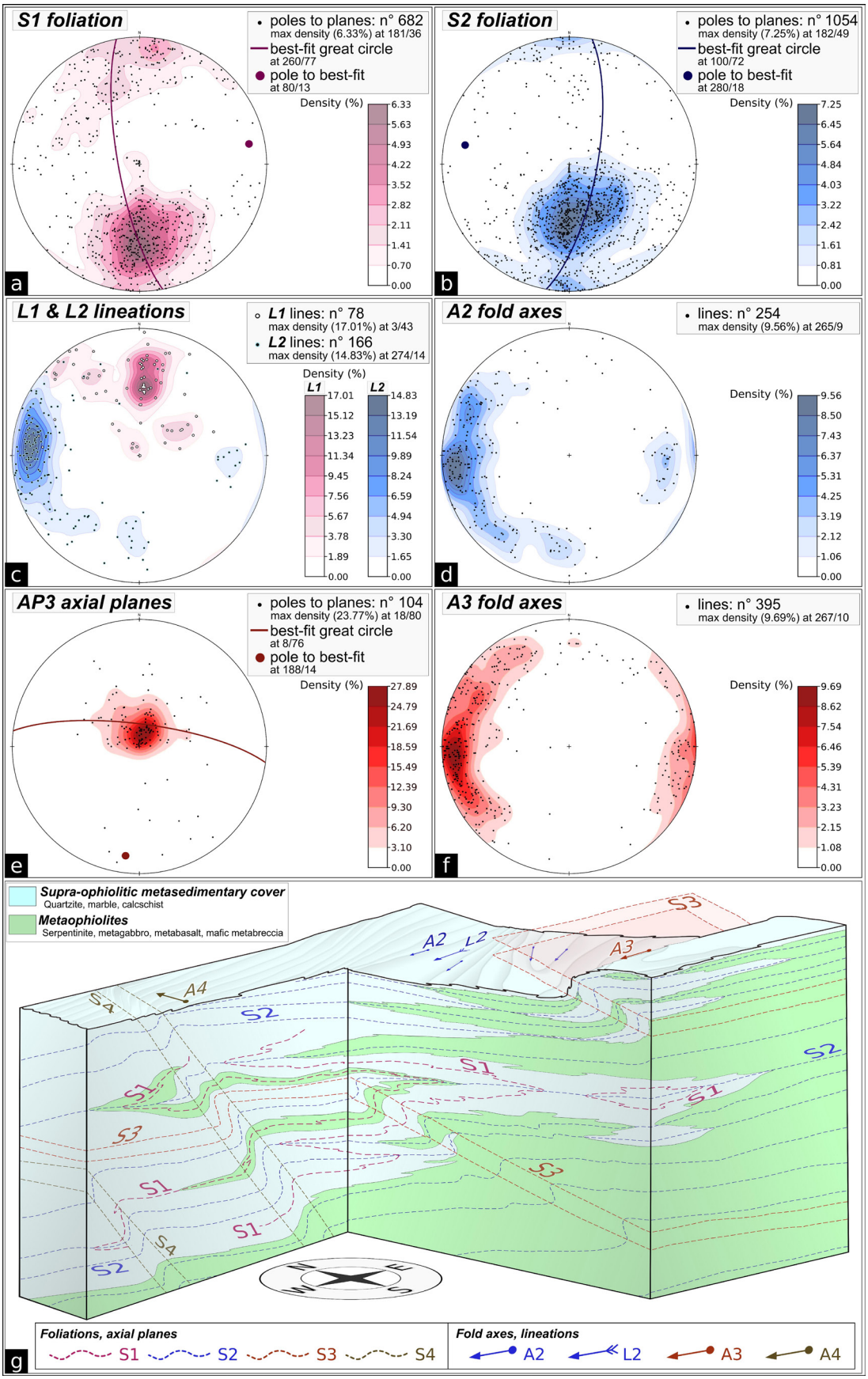

Fig. 4 - (a-f) Stereographic projections of mesoscale structural elements (Schmidt net, equal area, lower hemisphere; n°: data number; counting method: Fisher distribution; best-fit method: Bingham axial distribution). (g) Simplified 3D structural block-model of the geometrical superposing between structures of the different deformation phases. Two D1 folds are shown (note the eye-shaped anticline), folded by strongly non-cylindrical W-verging D2 folds, with anvil-shaped and eye-shaped folds (on the N-S surface). On the top of the model, A2 axes are shown (sub-)parallel to the L2 lineation. The superposed S1+S2 composite fabric is refolded by N-verging D3 folds and subsequent D4 folds.

ACKNOWLEDGEMENTS

The authors thank M. Maino and E. Sanità for their detailed reviews. A. Corno is also thanked for careful editorial handling. This research was funded by the University of Torino ("Ricerca Locale ex 60% 2020-2022"), and by the Italian Ministry of University and Research ("Cofin-PRIN 2020", grants no. 2020542ET7_003).

REFERENCES

Agard P. (2021) - Subduction of oceanic lithosphere in the Alps: Selective and archetypal from (slow-spreading) oceans. Earth Sci. Rev., 214, 103517.

Balestro G., Cadoppi P., Perrone G. & Tallone S. (2009) - Tectonic evolution along the Col del Lis-Trana Deformation Zone (internal Western Alps). It. J. Geosc., 128(2), 331-339.

Balestro G., Festa A., Borghi A., Castelli D., Gattiglio M. & Tartarotti P. (2018) - Role of Late Jurassic intra-oceanic structural inheritance in the Alpine tectonic evolution of the Monviso meta-ophiolite Complex (Western Alps). Geol. Mag., 155, 233-249.

Balestro G., Festa A. & Dilek Y. (2019) - Structural architecture of the Western Alpine ophiolites, and the Jurassic seafloor spreading tectonics of the Alpine Tethys. J. Geol. Soc. Lond, 176, 913-930.

Balestro G., Festa A., De Caroli S, Barbero E., Borghi A. & Gianotti F. (2022) - Multistage tectono-stratigraphic evolution of the Canavese Intracontinental Suture Zone: New constraints on the tectonics of the Inner Western Alps. Geosc. Front., 13(6), 101448.

Bearth, P. (1967) - Die Ophiolithe der Zone von Zermatt-Saas Fee. Beiträge zur Geologischen Karte der Schweiz. Neue Folge, 132, 130.

Caso F., Nerone S., Petroccia A. & Bonasera M. (2021) - Geology of the southern Gran Paradiso Massif and Lower Piedmont Zone contact area (middle Ala Valley, Western Alps, Italy). J. Maps, 17(2), 237-246.

Dal Piaz G.V., Bistacchi A., & Massironi M. (2003) - Geological outline of the Alps. Episodes, 26(3), 175-180.

De Togni M., Gattiglio M., Ghignone S. & Festa A. (2021) -Pre-Alpine tectonostratigraphic reconstruction of the Jurassic Tethys in the high-pressure Internal Piedmont Zone (Stura di Viù Valley, Western Alps). Minerals, 11(4), 361.

Festa A., Meneghini F., Balestro G., Pandolfi L., Tartarotti P., Dilek Y. & Marroni M. (2021) - Comparative analysis of the sedimentary cover units of the Jurassic Western tethys ophiolites in the Northern Apennines and Western Alps (Italy): Processes of the Formation of Mass-Transport and Chaotic Deposits during Seafloor Spreading and Subduction Zone Tectonics. J. Geol., 129(5), 533-561.

Gasco I., Gattiglio M. & Borghi A. (2011) - Lithostratigraphic setting and P–T metamorphic evolution for the Dora Maira Massif along the Piedmont Zone boundary middle Susa Valley, NW Alps. Int. J. Earth Sc., 100, 1065-1085.

Ghignone S., Gattiglio M., Balestro G. & Borghi A. (2020a) - Geology of the Susa Shear Zone (Susa Valley, Western Alps). J. Maps, 16(2), 1-8.

Ghignone S., Balestro G., Gattiglio M., & Borghi A. (2020b) - Structural evolution along the Susa Shear Zone: the role of a first-order shear zone in the exhumation of meta-ophiolite units (Western Alps). Swiss J. Geosci., 113(1), 1-16.

Ghignone S., Borghi A., Balestro G., Castelli D., Gattiglio M. & Groppo C. (2021a) - HP-tectono-metamorphic evolution of the Internal Piedmont Zone in Susa Valley (Western Alps): New petrologic insight from garnet+chloritoid -bearing micaschists and Fe-Ti metagabbro. J. Metamorph. Geol., 39, 391-416.

Ghignone S., Sudo M., Balestro G., Borghi A., Gattiglio M., Ferrero S., & van Schijndel V. (2021b) - Timing of exhumation of meta-ophiolite units in the Western Alps: New tectonic implications from 40Ar/39Ar white mica ages from Piedmont Zone (Susa Valley). Lithos, 404, 106443.

Handy M.R., Schmid S.M., Bousquet R., Kissling E. & Bernoulli D. (2010) - Reconciling plate-tectonic reconstructions of Alpine Tethys with the geological–geophysical record of spreading and subduction in the Alps. Earth Sc. Rev., 102, 121-158.

Herviou C., Agard P., Plunder A., Mendes K., Verlaguet A., Deldicque, D. & Cubaset N. (2021) - Subducted fragments of the Liguro-Piemont ocean, Western Alps: Spatial correlations and offscraping mechanisms during subduction. Tectonophysics, 827, 229-267.

Leardi L. & Rossetti P. (1985) - Caratteri geologici e petrografici delle Metaofioliti della Val d'Ala (Valli di Lanzo, Alpi Graie). Boll. Asso. Min. Sub. 22, 421-441.

Maino M., Adamuszek M., Schenker F. L., Seno S. & Dabrowski M. (2021) - Sheath fold development around deformable inclusions: Integration of field-analysis (Cima Lunga unit, Central Alps) and 3D numerical models. J. Struct. Geol., 144, 104255.

Manatschal M. & Müntener O. (2009) - A type sequence across an ancient magma-poor ocean-continent transition: the example of the Western Alpine Tethys ophiolites. Tectonophysics, 473, 4-19.

Nicolas A. (1969) - Tectonique et métamorphisme dans les Stura di Lanzo (Alpes Occidentales). Schweiz. Mineral. Petrogr. Mitteilungen, 49, 359-377.

Perotto A., Salino C., Pognante U., Genovese G. & Gosso G. (1983) - Assetto geologico-strutturale della Falda Piemontese nel settore dell'alta Valle di Viù (Alpi occidentali). Mem. Soc. Geol. It., 26, 479-483.

Plunder A., Agard P., Dubacq B., Chopin C. & Bellanger M. (2012) - How continuous and precise is the record of P-T paths? Insights from combined thermobarometry and thermodynamic modelling into subduction dynamics (Schistes Lustrés, W. Alps). J. Metamorph. Geol., 30, 323-346.

Ramsay J.G. (1962) - Interference patterns produced by the superposition of folds of similar type. J. Geol., 70(4), 466-481.

Rebay G., Zanoni D., Langone A., Luoni P., Tiepolo M. & Spalla M.I. (2018) - Dating of ultramafic rocks from the Western Alps ophiolites discloses Late Cretaceous subduction ages in the Zermatt-Saas Zone. Geol. Mag., 155, 298-315.

Rosenbaum G. & Lister G. (2005) - The Western Alps from the Jurassic to Oligocene: spatio-temporal constraints and evolutionary reconstructions. Earth-Sci. Rev., 69, 281-306.

Sandrone R., Leardi L., Rossetti P. & Compagnoni R. (1986) - P-T conditions for the eclogitic re-equilibration of the metaophiolites from Val d'Ala di Lanzo (internal Piemontese zone, Western Alps). J. Metamorph. Geol., 4, 161-178.

Spalla M.I., De Maria L., Gosso G., Miletto M. & Pognante U. (1983) - Deformazione e metamorfismo della Zona Sesia-Lanzo meridionale al contatto con la Falda Piemontese e con il Massiccio di Lanzo, Alpi Occidentali. Mem. Soc. Geol. It., 26, 499-514.

Tartarotti P., Guerini S., Rotondo F., Festa A., Balestro G., Bebout G.E., Cannaò E., Epstein S. & Scambelluri M. (2019) - Superposed sedimentary and tectonic block-in-matrix fabrics in a subducted serpentinite mélange (high-pressure Zermatt Saas Ophiolite, Western Alps). Geosciences, 9(8), 358.

Tricart P. & Schwartz S. (2006) - A north-south section across the Queyras Schistes lustrés (Piedmont zone, Western Alps): Syn-collision refolding of a subduction wedge. Ecl. Geol. Helv., 99, 429-442.